

# AN IN SITU REAL-TIME RBS STUDY OF SEQUENCE AND TEMPERATURE OF FORMATION OF NICKEL GERMANIDES

K.J. Pondo <sup>1,2,\*</sup>

<sup>1</sup> Department of Physics, University of Zambia, Lusaka 10101, Zambia

<sup>2</sup> Department of Physics, University of Cape Town, Rondebosch 7700, South Africa

\* Contact details: The University of Zambia, Institute of Distance Education, Box 32379, Lusaka, Zambia; Mobile: +260968799708;

e-mail: pondojk@yahoo.co.uk or [pondojk@gmail.com](mailto:pondojk@gmail.com) or [kanyembo.pondo@unza.zm](mailto:kanyembo.pondo@unza.zm)

---

*Accepted 16 October 2013*

## ABSTRACT

*The sequence of phase formation and the temperatures at which these phases form in the Ni/Ge binary system have been studied in real-time at sub-eutectic temperatures using in situ real-time Rutherford Backscattering Spectrometry (RBS). Nonconventional (i.e., with marker) thin film diffusion couples produced by depositing nanometric nickel films (47-80 nm) on Ge<100>-oriented substrates were thermally annealed in the scattering chamber by linear temperature ramping to induce solid phase reactions (SPR) between nickel and germanium. Only two phases were observed during the reaction. The first phase to nucleate was identified to be Ni<sub>5</sub>Ge<sub>3</sub> and its growth was observed at 145 °C. The last and final phase was found to be NiGe and its growth started at 170 °C. Although the growth of phases in the thin film diffusion couple regime is known to be sequential in which one phase grows before another phase starts to grow, an unusual simultaneous growth of Ni<sub>5</sub>Ge<sub>3</sub> and NiGe in the presence of nickel has been demonstrated in this study.*

**Keywords:** Nickel germanides, In situ real-time RBS, Ramped thermal anneal, Simultaneous growth.

## INTRODUCTION

Germanium and silicon are the best known elemental semiconductors and both belong to the same group in the Periodic Table. However, germanium (Ge) offers several attractive physical properties over silicon (Si). These include high saturated velocities of charge carriers of both polarities (electrons and holes) [1-4], very low carrier freeze-out temperatures, etc. The first property is the most advantageous over Si for deeply scaled metal-oxide-semiconductor field effect transistor (MOSFET) applications. Germanium had been historically one of the most important semiconductors in the past as the first MOSFET and integrated circuit (IC) were fabricated from Ge. However the

inferior properties of germanium dioxide (GeO<sub>2</sub>) as compared to silicon dioxide (SiO<sub>2</sub>) not only makes this dielectric unsuitable for Ge MOSFET gate insulation and field isolation, which has therefore obstructed very large scale integration (VLSI) realization in Ge for decades, but it also made Ge lose the race to Si as the semiconductor material of choice. The aggressive downscaling of devices is pushing the venerable SiO<sub>2</sub> to its performance limits since for ultrathin SiO<sub>2</sub> gate layers, of typical thickness below 3 nm [5], the gate dielectric breaks down and charge carriers can flow through the gate dielectric by the quantum mechanical tunneling mechanism [6, 7]. Therefore replacement of SiO<sub>2</sub> with higher permittivity (high-*k*) gate dielectrics [8] such as zirconia (ZrO<sub>2</sub>) or

hafnia ( $\text{HfO}_2$ ) which enable high gate capacitance with physically thick insulators through which tunneling is low has been proposed. Moreover, high- $k$  material based Ge MOSFETs with germanium oxynitride, zirconia and hafnia gate dielectrics have been successfully demonstrated [4, 9, 10]. The replacement of thermally grown  $\text{SiO}_2$  by high- $k$  materials as new gate dielectrics in complementary metal-oxide-semiconductor (CMOS) devices has eliminated one of silicon's technological advantages (its remarkable oxide no longer being used as a gate insulator) and has also overcome the major drawback Ge oxide initially faced. Consequently, Ge is an appealing alternative semiconductor material and is a possible replacement for Si. This has renewed interest in understanding the structure, stability and physical properties of metal germanides. Metal germanides have great potential for applications in nano/microelectronics, optoelectronics and solid state detectors.

Before germanium can be adopted, a suitable material for making electrical contacts to the active areas of the germanium based devices must be identified. In analogy with the current Si-based technology where metal-silicides are used as contacts, the use of metal-germanides is proposed for this purpose. Of all possible metal-germanides, nickel monogermanide ( $\text{NiGe}$ ) appears to be the most promising [11]. In order to successfully make use of nickel germanides in Ge-based devices it is essential to thoroughly understand all processes and mechanisms involved in germanium metallization as well as the properties of the phases formed. Identification of the sequence of formation of the phases and temperatures at which they are formed during the germanidation process is among the important pieces of information required during fabrication. This is important in industrial applications where it determines the heat treatment required to obtain a unique targeted phase with specific properties.

In thin film reactions only some of the compounds present on the equilibrium binary

phase diagram form during solid state reactions. The available reports on thin film work for the Ni/Ge system indicate that only two phases are observed. They agree on the second and final phase,  $\text{NiGe}$ , but disagree on the first phase. Some researchers report orthorhombic  $\text{Ni}_2\text{Ge}$  [12-14] while others report monoclinic  $\text{Ni}_5\text{Ge}_3$  [15-19] or hexagonal  $\text{Ni}_3\text{Ge}_2$  [20] as the first phase to form.

In this work, we report a study of the formation of nickel germanides obtained by solid state reaction. The phase formation sequence and the temperatures at which the phases form are the main focus of the work reported here.

## EXPERIMENTAL DETAILS

A 5-Å layer of tantalum (Ta) and an 800-Å layer of nickel (Ni) were sequentially electron beam evaporated on a  $\langle 100 \rangle$ -oriented germanium (Ge) substrate at room temperature to obtain a sample with a trilayer structure  $\text{Ge}\langle 100 \rangle/\text{Ta}(5 \text{ \AA})/\text{Ni}(800 \text{ \AA})$ . The base pressure during electron beam vacuum evaporation was kept in the low  $10^{-7}$  torr region.

The sample was then mounted on the flat surface of a copper heating stage with highly conductive silver adhesive paste. A thermocouple was mounted from the rear through a narrow hole drilled in the copper block so that the tip was located just underneath the copper surface. By measuring the surface resistance of the two simple systems Au-Si and Al-Si with eutectic temperatures of 363 °C and 577 °C respectively as a function of the thermocouple temperature, a calibration curve was obtained which could then be used to estimate the sample surface temperature from the measured resistance. The heating stage was shielded from the chamber by an air-cooled heat sink to minimize unwanted heating of the chamber. With the addition of a liquid nitrogen cold panel, the annealing could be carried out at a pressure of about  $4 \times 10^{-6}$  Torr.

The sample was annealed and analyzed in situ in the Rutherford Backscattering Spectrometry (RBS) chamber by linear temperature ramping to induce solid state reactions of Ni with Ge. The investigation was carried out in a temperature range from 20 °C to 350 °C as recorded by the thermocouple.

RBS spectra were obtained with 2 MeV He<sup>+</sup> particles using a backscattering angle of 165° and tilting the sample normal 50° away from the incident beam. The RBS spectra were acquired continuously and accumulated spectra stored at regular intervals of 30 s. The acquired charge and recorded sample temperatures were also saved with each spectrum in an event by event mode which could subsequently be played back for analysis.

When processing the data after the run had completed, the spectra were summed up into appropriate time intervals, e.g., 2 or 4 min and charge normalized. In this study the individual spectra were analyzed using the RUMP-code and semi-automatic PERT-subroutine [21, 22].

## RESULTS AND DISCUSSION

To determine the sequence of phase formation and the temperatures at which these phases form in the thin-film Ni/Ge system the trilayer Ge<100>/Ta(5 Å)/Ni(800 Å) was annealed in the RBS scattering chamber by linearly ramping the temperature from 20 °C to 350 °C (thermocouple temperature) in order to induce solid-phase reaction (SPR) of Ni with Ge. Studies by Marshal et al. [10] and Gaudet et al. [9] show that Ta does not react with Ge to form any compounds in this temperature range. It should be noted that the thin layer of Ta interposed between the Ni and Ge substrate was only used as an inert marker to monitor the direction of atomic mobility in a related study not reported here [23].

The *in situ* real-time RBS results obtained when the above trilayer was annealed revealed that only two phases form in the Ni/Ge

system. The reaction commenced around 145 °C with the formation of the Ni<sub>5</sub>Ge<sub>3</sub> as the initial phase. At around 170 °C a new phase appeared and it was identified using RUMP to be NiGe. The formation of this second and final phase started even before all the Ni had been completely consumed. The growth and decomposition of the Ni<sub>5</sub>Ge<sub>3</sub> and the NiGe phases together with the consumption of Ni are presented schematically in Figure 1 which shows the thicknesses of the Ni, Ni<sub>5</sub>Ge<sub>3</sub> and NiGe layers as a function of the annealing temperature with all quantities expressed in terms of the number of Ni atoms ( $\times 10^{15}$  Ni at/cm<sup>2</sup>) present in each phase. In this way the consumption of Ni, the growth and decomposition of Ni<sub>5</sub>Ge<sub>3</sub>, as well the formation of the NiGe phase throughout the reaction can be more easily seen. Therefore, Figure 1 represents the various phases present at each stage of the reaction in terms of the number of Ni atoms in each phase.

Although the growth of phases in thin film solid state reactions is known to be sequential, in which one phase grows before another phase can start to grow, Figure 1 demonstrates an unusual simultaneous growth of the Ni<sub>5</sub>Ge<sub>3</sub> and NiGe phases in the presence of Ni from the onset of NiGe growth up to 298 °C when the Ni<sub>5</sub>Ge<sub>3</sub> phase started to decompose.

It can be seen from Figure 1 that the growth of the Ni<sub>5</sub>Ge<sub>3</sub> phase was steady from its nucleation up to the time it started to decompose. On the other hand Figure 1 shows that the formation of NiGe is characterized by a change in the growth rate. The growth of the NiGe phase can be observed to be steady from its nucleation temperature up to 254 °C. It then started to decompose between 255 °C and 272 °C. However the NiGe did not decompose completely as no further decomposition of this phase was observed between 272 °C and 298 °C. Instead the NiGe phase maintained an almost constant thickness of about  $54 \times 10^{15}$  at/cm<sup>2</sup> in this temperature window. The NiGe phase then started growing with a much faster growth rate from 298 °C by the consumption of Ni<sub>5</sub>Ge<sub>3</sub> through a thermal decomposition

mechanism until the end of the reaction. The decomposition of the NiGe phase between 255 °C and 272 °C is quite strange and the reasons for this are not very clear. It might seem that as the Ni<sub>5</sub>Ge<sub>3</sub> and NiGe phases grew simultaneously there was phase competition between the two phases which favored the growth of the former phase and forced the latter phase to decompose to a certain thickness which it maintained until the former phase started to decompose. Although the simultaneous growth of Ni<sub>5</sub>Ge<sub>3</sub> and NiGe demonstrated in Figure 1 deviates from the sequential formation usually observed during solid state reactions in thin films [24], this behavior is supported by the results reported in other studies [15-17].

The suitability of in situ real-time RBS (i.e., RBS spectra are collected at regular intervals of time during annealing) is demonstrated in Figure 1 where the real-time RBS data have allowed a quantitative analysis of the germanide thin film growth. The numerous data points the real-time method inherently generates for each of the phases allow complete characterization of phase evolution and in this way both reactions, i.e., the formation of Ni<sub>5</sub>Ge<sub>3</sub> and the formation of NiGe, could be properly distinguished.

The RBS plot in Figure 2 illustrates a schematic set-up of RBS and an example of an energy spectrum for two-element thin film on a Ge<100> oriented substrate of the virgin spectrum.

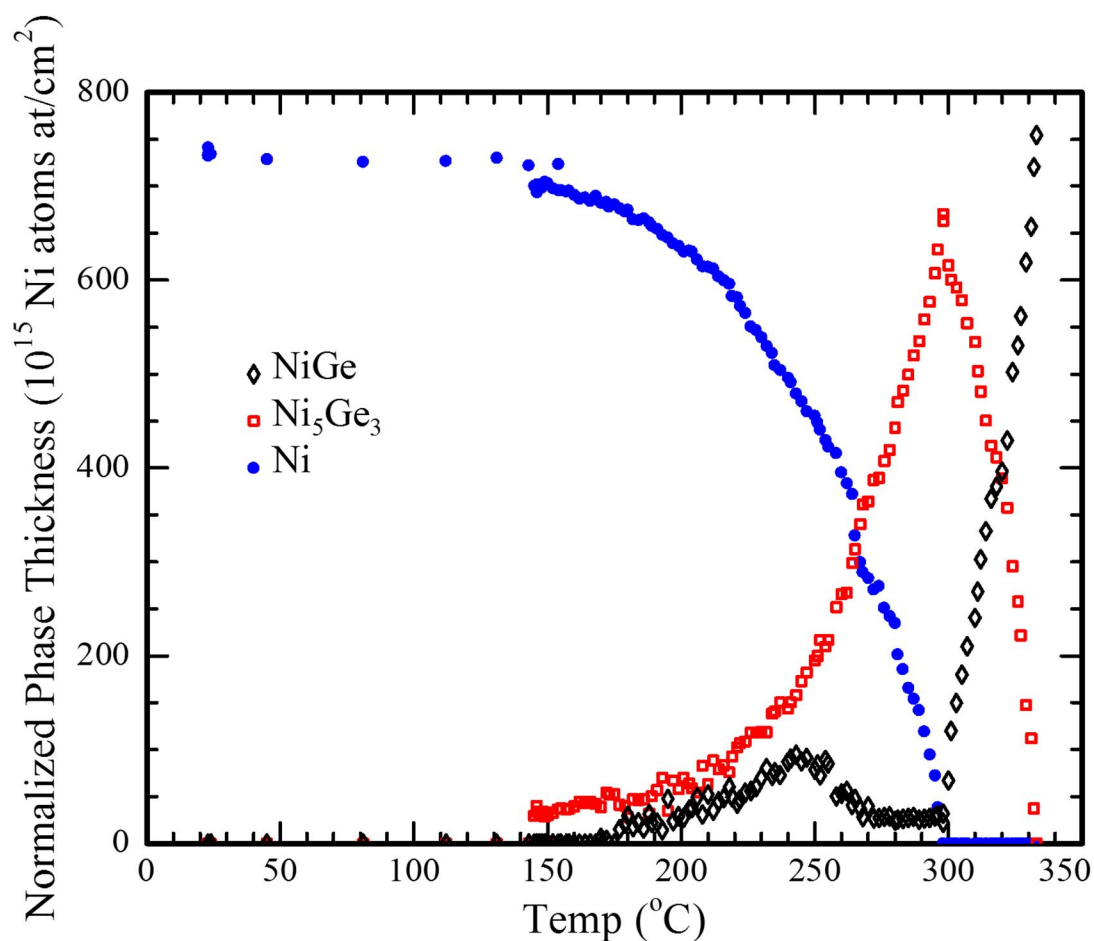


**Figure 1:** Overview of the evolution and decomposition of phases during linear ramped annealing of an 80 nm thick Ni film deposited on Ge<100> substrate.

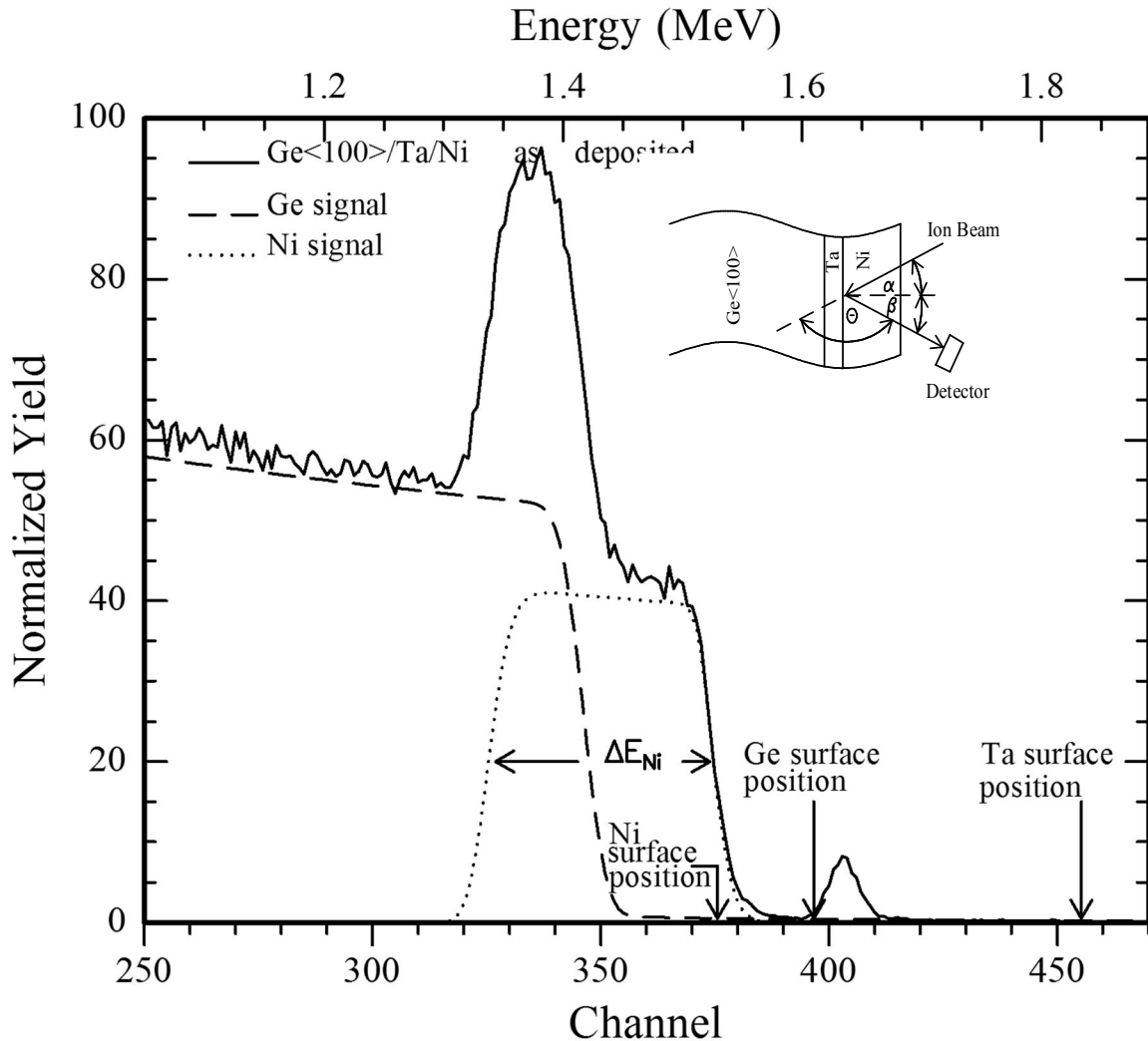


**Figure 2:** MeV  $^4\text{He}^+$  backscattering energy spectrum from an as-deposited sample obtained by first electron beam evaporating 5 Å of tantalum on a  $\langle 100 \rangle$ -oriented germanium substrate and finally electron beam evaporating 800 Å of nickel on top of the tantalum. The simulated contributions of the Ni (dotted line) and Ge (dashed line) signals included in the RBS spectrum are useful in revealing spectral features that might not be immediately apparent.  $\Delta E_{\text{Ni}}$  is the energy difference between the energy of the alpha particles scattered from the Ni atoms at the surface and the energy of the alpha particles scattered from the Ni atoms at the Ni/Ta interface. The inset shows the sample structure and schematic set-up of RBS.

Figure 2 has been included as a useful aid in understanding the energy spectra of Ta and Ni deposited on a Ge substrate. The ions scattered from each element form a separate peak. The number of target atoms in the film can be derived from the peak yields and the peak width gives the film thickness. The surface positions of Ta, Ge and Ni (i.e. position where the signal would appear if the elements were at the surface) and the simulated contribution of the Ni and Ge

signals to the RBS spectrum are also shown in Figure 2. From the schematic insert one can see that only Ni is at the surface and thus only the Ni RBS peak appears at its surface position. Only particles scattered from the surface of the Ni film have an energy given by the surface position of the Ni. As particles traverse the solid, they lose energy along the incident path. Particles scattered from Ni atoms at the Ta-Ni interface therefore have energies less than the surface energy of Ni. On

the outward path the particles again lose energy. On emerging from the surface, the particles scattered at the Ta-Ni interface have a total energy difference  $\Delta E_{\text{Ni}}$  from the particles scattered at the surface.

Since there are no Ta atoms at the surface position, the peak produced by scattering from Ta starts at a lower energy than the surface energy of Ta. However the tantalum signal is well separated from the signals of Ni and Ge because even though it is buried the atomic mass of Ta is much larger than those of both Ni and Ge.

As there are no Ge atoms on the surface, the peak produced by scattering from Ge also starts at an energy lower than the surface energy of Ge and then extends to zero energy because Ge atoms form a substrate with an effectively infinite thickness. By simulating the Ni and Ge peaks separately (dotted and dashed lines in Figure 2 respectively), it is easy to see how the overlap between the front of the Ge signal and the back of the Ni signal gives rise to the peak which appears to rise above a continuous background. It must be emphasized that this peak is not due to the superposition of a peak on a continuous background (as for example an oxygen peak on a silicon background in  $\text{SiO}_2$ ) but is rather from the overlap of two signals, and that the background at the back is that from Ge, while that in front arises from Ni (and so the background is in no way “continuous”).

In general, for surface analysis by RBS, conditions must be such that the mass of surface atoms is considerably higher than the mass of the substrate atoms if the peak arising from the surface atoms is to be completely resolved. Nevertheless, the use of the RUMP program allowed this problem to be circumvented when analyzing our RBS spectra.

Four of the RBS spectra acquired during the in situ real-time RBS measurement taken at selected stages of the SPR are presented in Figure 3. These spectra were selected to

illustrate the as-deposited spectrum at room temperature, the spectrum at the beginning of  $\text{Ni}_5\text{Ge}_3$  growth around 145 °C, the onset of NiGe formation around 170 °C, the stage at which all the Ni is totally consumed and the spectrum at the end of the reaction at 333 °C. In Figure 3 the virgin spectrum (as-deposited), the spectrum taken at the start of  $\text{Ni}_5\text{Ge}_3$  growth and the spectrum captured around the onset of NiGe growth almost overlap. However, careful examination of the Ta marker signal in the three spectra reveals a slight displacement of the Ta signals in the three spectra which indicates that the reaction had already started taking place. The spectra up to these three stages of the SPR appear almost the same because so far only very little of the surface Ni is consumed in the formation of  $\text{Ni}_5\text{Ge}_3$  and NiGe. This means that the amount of Ni and Ge in these compounds is equally small so that the overall shape of each of the three energy spectra is predominantly due to the overlap of the unreacted surface Ni and the Ge in the substrate. However as can be seen from the spectrum illustrating the total consumption of Ni and the one at the end of the reaction, the shape of the energy spectra change markedly as the surface Ni become thinner and as the amount of Ni and Ge in the grown compounds increase. It must also be noted that the Ta signals in the spectrum captured when the Ni is totally consumed and the one at the end of the reaction overlap because at this stage of the reaction all the Ta has now moved to the surface of the sample [23].

The spectra in Figure 3, except the spectrum taken when all the Ni was totally consumed, are presented individually in Figure 4 corroborated with their RUMP simulations to show agreement between the measured spectra and their simulations.

The NiGe film remained stable until the end of the annealing. The temperature was held constant at 333 °C (350 °C thermocouple temperature) for a further 40 min but no formation of new phases was observed.

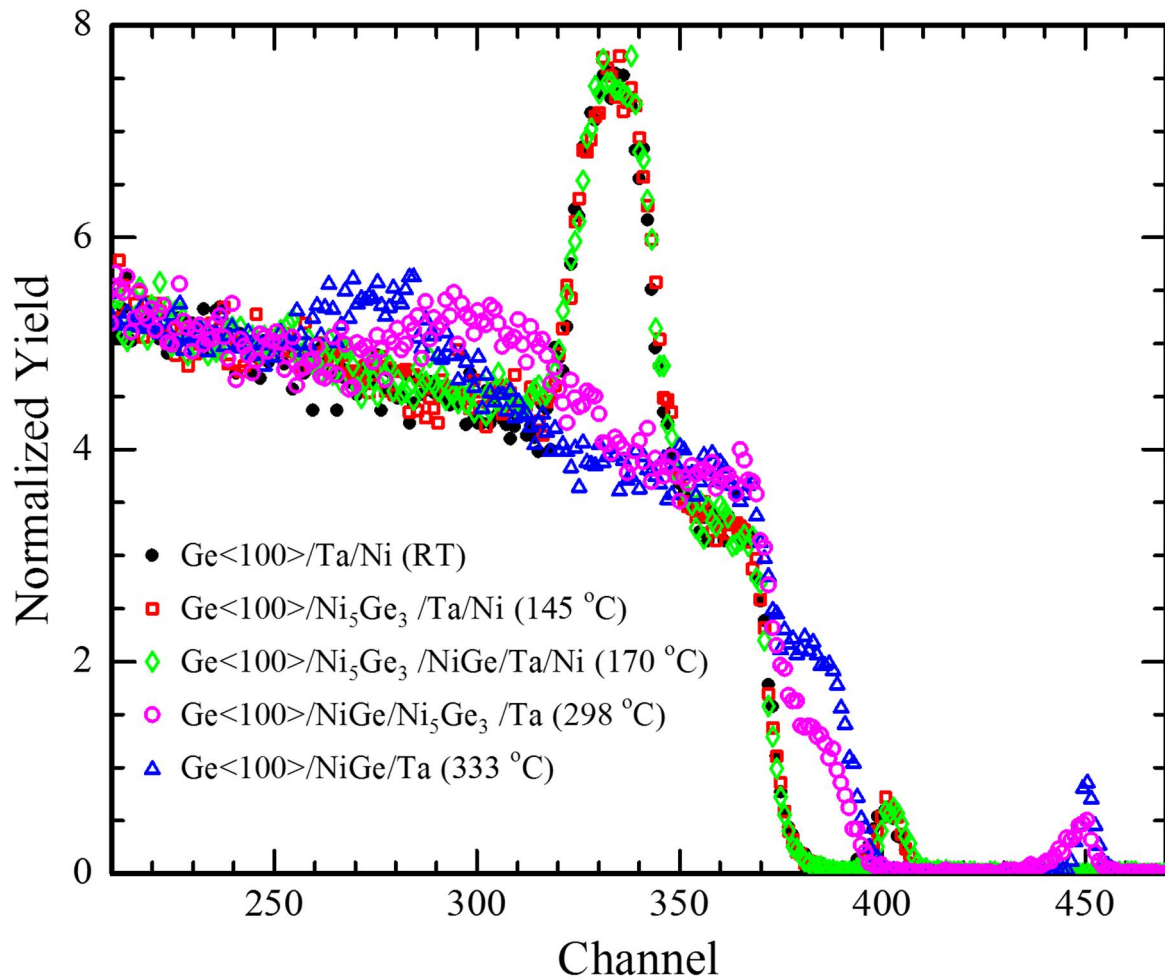


**Figure 3:** Selected RBS spectra acquired during real-time RBS measurement of an 80 nm thin Ni film on Ge<100> at several stages of the solid-phase reaction, i.e. as deposited (at RT, solid circles), during onset of Ni<sub>5</sub>Ge<sub>3</sub> growth (at 145 °C, squares), during the onset of NiGe formation (at 287 °C, diamonds), when all the surface Ni is totally consumed (298 °C, open circles) and the spectrum at the end of the reaction (at 333 °C, triangles).

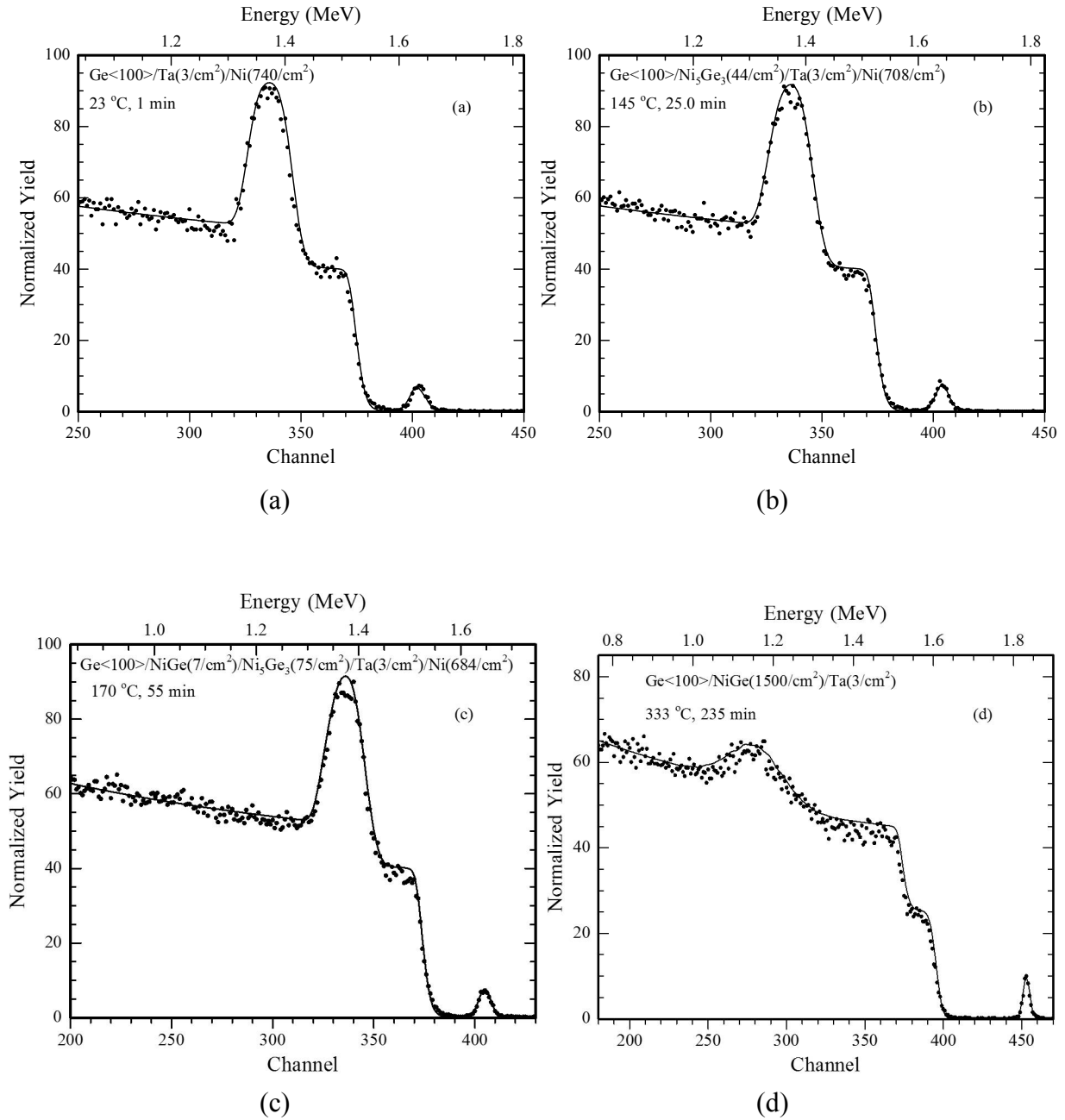


**Figure 4:** The spectra in Figure 3 with their RUMP simulations. The spectrum in (a) is from the as-deposited sample, (b) shows the onset of  $\text{Ni}_5\text{Ge}_3$  formation, (c) shows the onset of  $\text{NiGe}$  formation and (d) is the spectrum at the end of the reaction. The temperature and time period of annealing at which each spectrum was taken are also indicated. The thicknesses are in units of  $10^{15}$  atoms/ $\text{cm}^2$ .

This indicates that  $\text{NiGe}$  is the last germanium rich phase that forms during the SPR of Ni with Ge. This agrees with the Ni-Ge binary

equilibrium phase diagram [25] (Figure 5) where  $\text{NiGe}$  is predicted as the last and most Ge-rich phase to form in the Ni/Ge system.

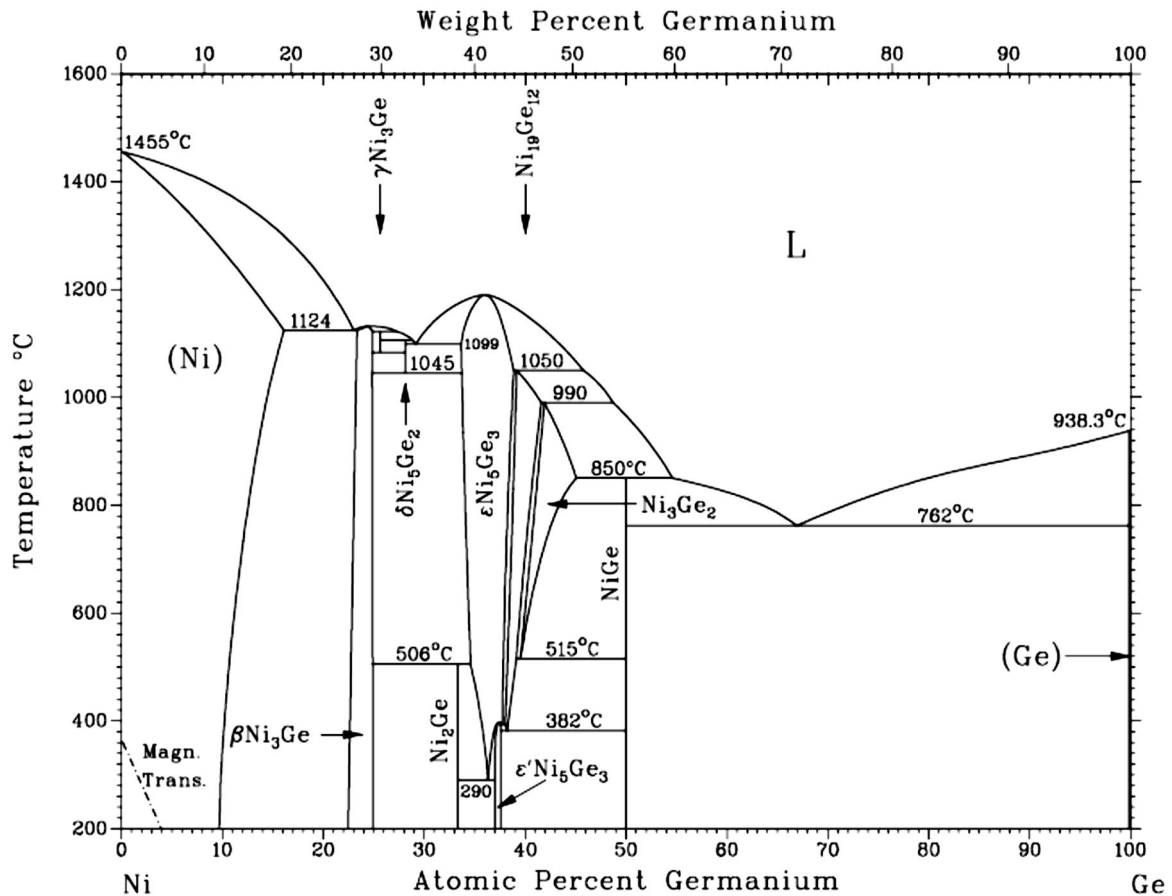


**Figure 5:** The Ni-Ge binary equilibrium phase diagram [25].

By adding the third dimension of either time or temperature, it is possible to plot the spectra for the complete reaction as a single 3 dimensional plot. Since temperature was held constant at 333 °C for several minutes, time was chosen as the third dimension for the 3-D plot presented in Figure 6. It can be seen from Figure 6 that from the point where the Ni and Ge peaks start splitting one peak moves to the left while the other moves to the right. Figure 7 has been included in order to explain how the splitting of peaks forming the two ridges moving in opposite directions comes about. Two individual spectra captured during the run are shown in Figure 7, namely the spectrum captured at 43 °C (which is similar

in form to the spectrum in Figure 2 since little reaction occurs before 150 °C) and one captured at a temperature of around 267 °C. The single peak in the spectrum captured at 43 °C (solid line) arises from the overlap of the Ni and Ge signals as explained earlier. As the reaction progresses the Ni moves deeper into the sample making the layer of Ni above the Ta marker thinner. As a result of this thinning of the Ni layer above the Ta, the Ge in the growing germanides appears at higher channels while the Ni in the growing germanides appears at lower channels. This in turn causes the single peak to split into two peaks which are clearly visible in the 267 °C spectrum.

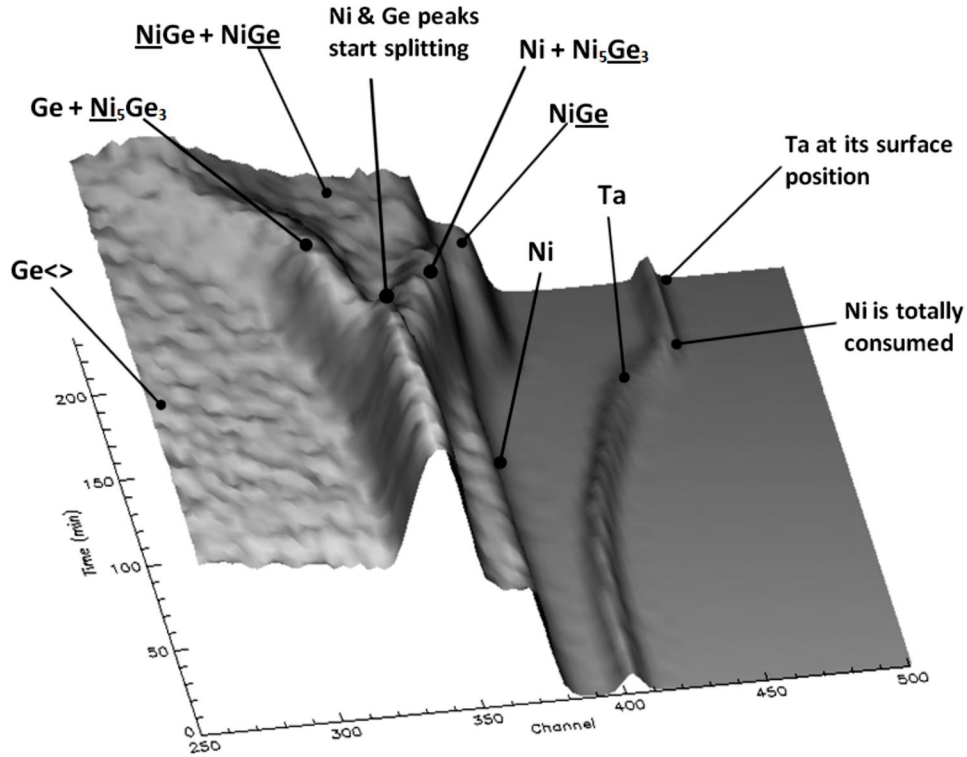


**Figure 6:** In situ, real-time RBS spectra of the formation of  $\text{Ni}_5\text{Ge}_3$  and  $\text{NiGe}$  for the sample with configuration  $\text{Ge}\langle 100 \rangle / \text{Ta}(5 \text{ \AA}) / \text{Ni}(800 \text{ \AA})$ . The Ta marker interposed between the Ge substrate and Ni layer shifts to higher energies throughout the reaction.

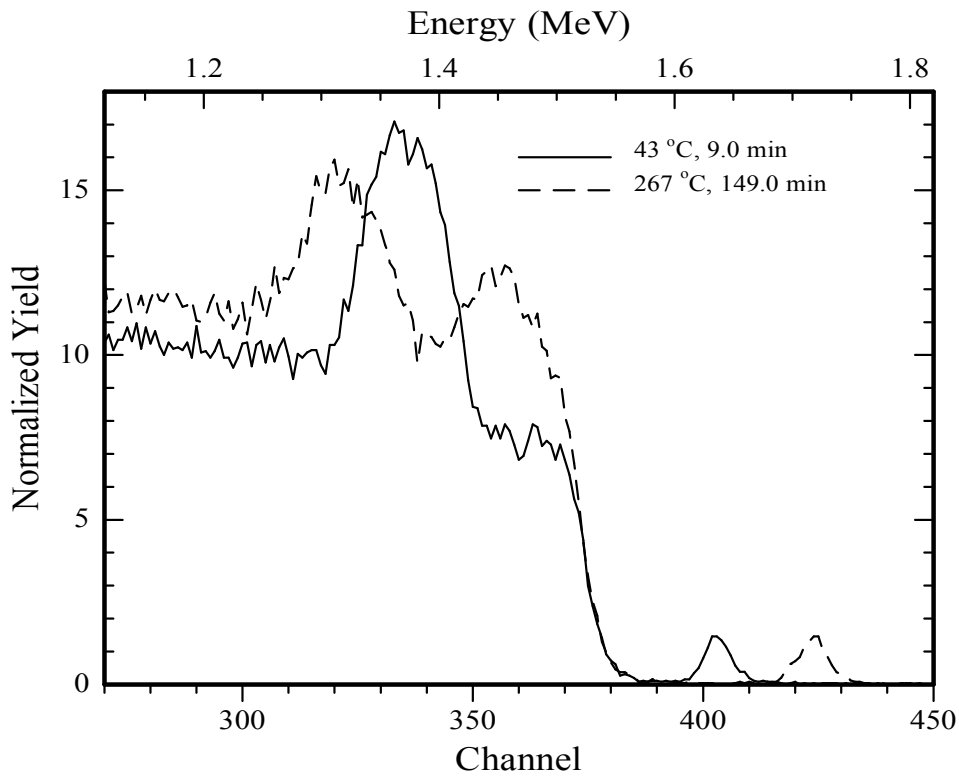


**Figure 7:** In situ, real-time RBS showing a spectrum captured before the splitting of Ni and Ge peaks (solid Line) and another spectrum captured after splitting of the peaks (dashed line).

The spectrum captured at a temperature of around 267 °C is again presented in Figure 8 with the simulated contributions of the Ni (dashed line) and Ge (dotted line) signals. The kink in the leading (front) edge of the Ge signals represents the Ge atoms in the growing germanides while the kink in the back edge of the Ni signal represents the Ni atoms in the growing germanides. Therefore, the peak on the left in Figure 8 arises from the overlap of the Ni in the growing germanides and the Ge in the substrate while the peak on the right arises from the overlap of the Ge in the growing germanides and the unreacted surface Ni. Therefore, the plot given in Figure

8 is especially useful to gain an intuitive feeling for complex overlapping spectra.

By comparing the positions of the front edge of the simulated Ge signal and the back edge of the simulated Ni signal in Figure 2 with the positions of these edges in Figure 8 it can be seen that these edges have moved to higher and lower channels respectively. By using the split command of the RUMP code it was possible to identify the contributions of Ni and Ge to the various features appearing in Figure 6. Thus the underlined element in Figure 6 such as in NiGe shows that the indicated feature results from the Ge in the NiGe phase and so on.

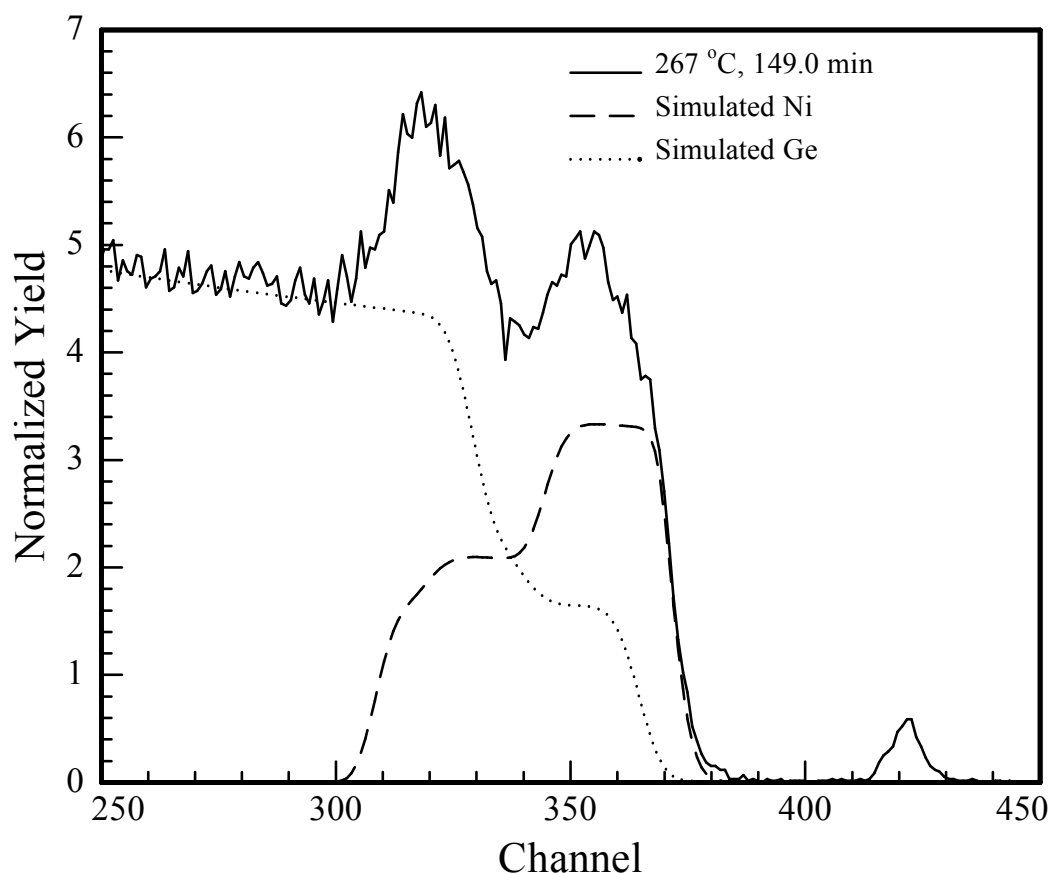


**Figure 8:** In situ, real-time RBS showing a spectrum captured at around 267 °C after the splitting of Ni and Ge peaks had already begun. The simulated contributions of the Ni (dashed line) and Ge (dotted line) signals to this spectrum are also included.

The spectrum in Figure 9 was taken at 350 °C (thermocouple temperature) and is very helpful in illustrating how the feature labeled NiGe in Figure 6 is produced. From the simulated contributions of the Ni and Ge signals to the spectrum presented in Figure 9 it is easy to see that at this stage of the reaction the Ni signal is entirely under the Ge signal with the leading edge of the Ni signal well behind the leading edge of the Ge signal. Therefore the feature labeled NiGe in Figure 6 results from the Ge in the NiGe phase. The 3-D plot presented in Figure 6 is therefore a graphical illustration of the complex overlap

of the Ni and Ge signals that occur at different stages of the reaction in the Ni/Ge system.

The surface position of Ta is 453.457 in terms of channel number which is equivalent to 1.833 MeV in terms of the energy. It can be seen from Figure 6 that the position at which the Ta stopped moving coincides with this energy. This means that all the Ta atoms diffused to the surface of the sample resulting in an interlayer inversion between the Ni which was initially at the surface of sample and the Ta which was initially buried beneath the Ni atoms.

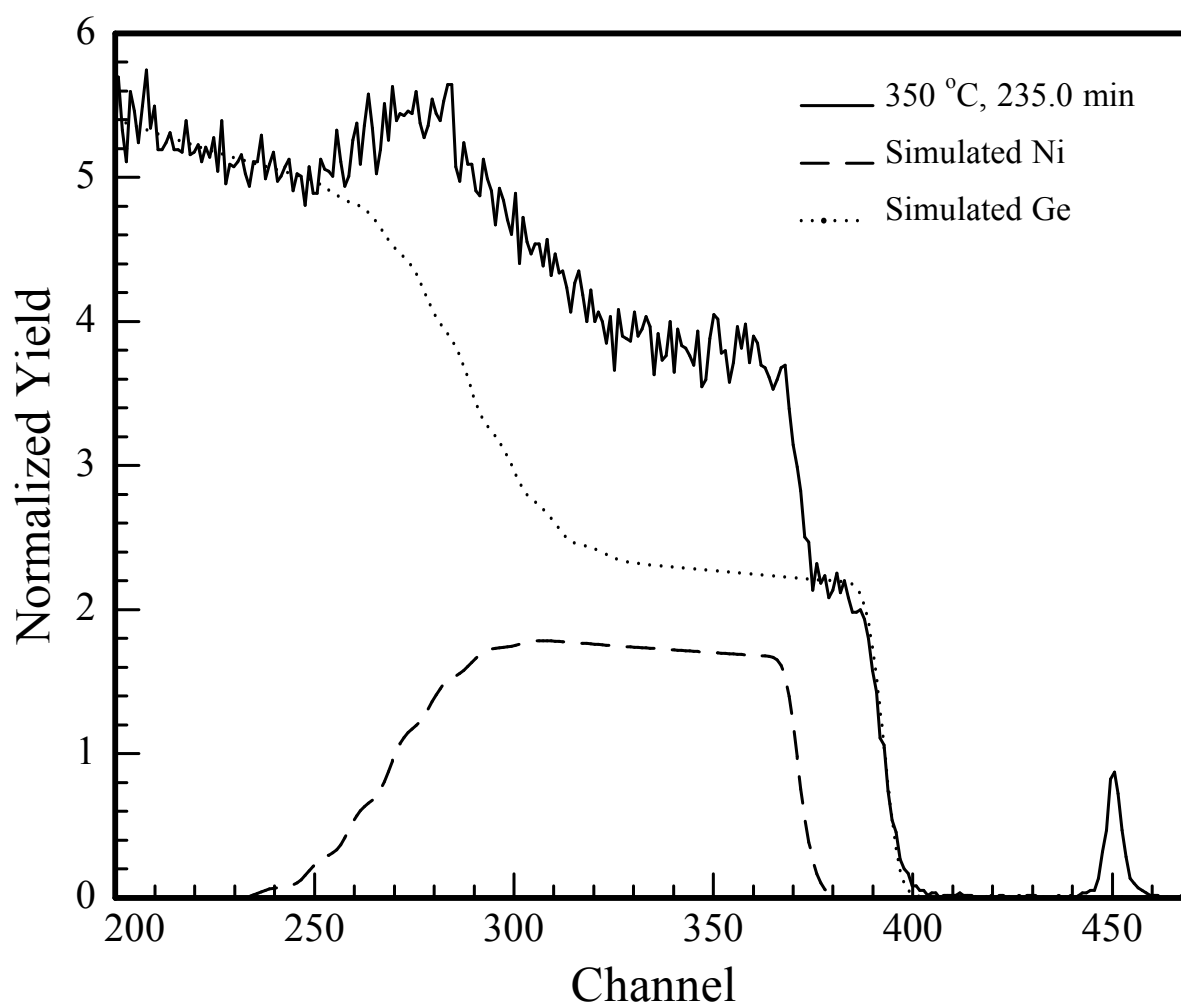


**Figure 9:** In situ, real-time RBS showing a spectrum captured at around 350 °C (as recorded by the thermocouple) illustrating how the feature labeled NiGe in Figure 6 is produced.

## CONCLUSION

According to the present study, the following conclusions can be drawn:

1. The Ni-rich phase that forms first during the solid-state reaction of Ni thin film with Ge was found to be Ni<sub>5</sub>Ge<sub>3</sub>. Thus the phase formation sequence in the Ni/Ge system has been found to be Ni<sub>5</sub>Ge<sub>3</sub> followed by NiGe as the last and final phase;
2. The temperatures at which formation of the Ni<sub>5</sub>Ge<sub>3</sub> and NiGe phases were observed were found to be 145 °C and 170 °C respectively. The inferior thermal stability and water solubility of GeO<sub>2</sub> which hinder the real application of Ge MOSFET [26] can be overcome by the use of high-*k* gate dielectric materials. Therefore, the low temperature germanidation observed in the present study is advantageous for the effective prevention of the degradation of the high-*k* gate stack on germanium substrate and this makes nickel germanide more suitable for Ge device fabrication;
3. Finally, it has been shown that the growths of Ni<sub>5</sub>Ge<sub>3</sub> and NiGe are simultaneous and not sequential as usually observed in thin films.

## ACKNOWLEDGMENTS

The author wishes to gratefully thank Prof. C.M. Comrie of the University of Cape Town and Dr. A. Habanyama of the University of Zambia for their meticulous supervision of the dissertation from which this work is derived. The author is also greatly indebted to the University of Zambia where the MSc was offered and the University of Cape Town for hosting him during the research part of his studies. The author further wishes to thank the Materials Research Group at the iThemba Labs (formally the National Accelerator Center at Faure) for the use of their facilities

and materials. It is also a sincere wish of the author to greatly acknowledge the financial support of the International Science Program (ISP) for his MSc and the former course coordinator Dr. G.K. Chinyama (Chartered Physicist) for introducing the MSc course in Materials Science in the Physics Department of the University of Zambia.

## REFERENCES

- [1] C.O. Chui, H. Kim, D. Chi, B.B. Triplett, P.C. McIntyre, and K.C. Saraswat, "A sub-400 °C germanium MOSFET technology with high-*k* dielectric and metal gate," *IEDM Tech. Dig.*, (2002) 437–440.
- [2] A. Ritenour, S. Yu, M.L. Lee, N. Lu, W. Bai, A. Pitera, E.A. Fitzgerald, D.L. Kwong, and D.A. Antoniadis, "Epitaxial strained germanium p-MOSFETs with HfO<sub>2</sub> gate dielectric and TaN gate electrode", *IEDM Tech. Dig.*, (2003) 433–436.
- [3] H. Shang, H. Okorn-Schmidt, K.K. Chan, M. Copel, J. A. Ott, P.M. Kozlowski, S.E. Steen, S.A. Cordes, H.-S. P. Wong, E.C. Jones, and W.E. Haensch, "High mobility p-channel germanium MOSFETs with a thin Ge oxynitride gate dielectric", *IEDM Tech. Dig.*, (2002) 441–444.
- [4] C.O. Chui, S. Ramanathan, B.B. Triplett, P.C. McIntyre, and K.C. Saraswat, "Germanium MOS Capacitors Incorporating Ultrathin High-*k* Gate Dielectrics", *IEEE Electron Device Lett.*, **23** (8) (2002) 473-475.
- [5] Michel Houssa and Marc Heyns, 2004. "High-*k* gate dielectrics: why do we need them?" In: *High-*k* Gate Dielectrics*, Michel Houssa (ed), 3-14, Bristol and Philadelphia: Institute of Physics Publishing.

- [6] M. Depas, B. Vermeire, P.W. Mertens, R.L. Van Meirhaeghe and M.M. Heyns, "Determination of tunnelling parameters in ultra-thin oxide layer poly-Si/SiO<sub>2</sub>/Si structures", *Solid-State Electron.*, **38** (8) (1995) 1465-1471.
- [7] S.H. Lo, D.A. Buchanan, Y. Taur and W. Wang, "Quantum-mechanical modeling of electron tunneling current from the inversion layer of ultra-thin-oxide nMOSFET's", *IEEE Electron. Dev. Lett.*, **18** (1997) 209-211.
- [8] G. D. Wilk, R. M. Wallace, and J. M. Anthony, "High-k gate dielectrics: Current status and materials properties considerations," *J. Appl. Phys.*, **89** (10) (2001) 5243-5275.
- [9] H. Shang, K.L. Lee, P. Koslowski, C. D'Emic, I. Babich, E. Sikorshi, M. Jeong, H.S.P. Wong, K. Guarini and W. Haensch, "Self-aligned n-channel germanium MOSFETs with a thin Ge oxynitride gate dielectric and tungsten gate", *IEEE Electronic Device Lett.*, **25** (3) (2004) 135-137.
- [10] H. Shang, H. Okorn-Schmidt, K.K. Chan, M. Copel, J.A. Ott, P.M. Koslowski, S.E. Steen, S.A. Cordes, H.S.P. Wong, E.C. Jones and W.E. Haensch, "High mobility p-channel Germanium MOSFETs with a thin Ge oxynitride gate dielectric", *IEDM Tech Dig.*, (2002) 441-444.
- [11] S. Gaudet, C. Detavernier, A.J. Kelioc, P. Desjardins and C. Lavoie. "Thin film reaction of transition metals with germanium", *J. Vac. Sci. Technol. A* **24** (3) (2006) 474-485.
- [12] E. D. Marshall, C. S. Wu, C. S. Pai, D. M. Scott and S. S. Lau, "Metal-Germanium Contacts and Germanide Formation", *Mater. Res. Soc. Symp. Proc.*, **47** (1985) 161-166.
- [13] Y.F. Hsieh, L.J. Chen, E.D. Marshall, S.S. Lau and N. Kawasaki, "Partial epitaxial growth of Ni<sub>2</sub>Ge and NiGe on Ge(111)", *Thin Solid films*, **162** (1988) 287-294.
- [14] M.W. Wittmer, M.-A. Nicolet and J.W. Mayer, "The First Phase to Nucleate in Planar Transition Metal-Germanium Interfaces", *Thin Solid Films*, **42** (1977) 51-59.
- [15] S. Gaudet, C. Detavernier, A.J. Kelioc, P. Desjardins and C. Lavoie. "Thin film reaction of transition metals with germanium", *J. Vac. Sci. Technol. A* **24** (3) (2006) 474-485.
- [16] F. Nemouchi, D. Mangelinck, J.L. Lábár, M. Putero, C. Bergman and P. Gas, "A comparative study of nickel silicides and nickel germanides: Phase formation and kinetics", *Micro Electronic Engineering*, **83** (2006) 2101-2106.
- [17] F. Nemouchi, D. Mangelinck. C. Bergman, G. Clugnet and P. Gas, "Simultaneous growth of Ni<sub>5</sub>Ge<sub>3</sub> and NiGe by reaction of Ni films with Ge", *Appl. Phys. Lett.*, **89** (2006) 131920.
- [18] J. Ken Patterson, B.J. Park, K. Ritley, H.Z. Xiao, L.H. Allen and A. Rockett, "Kinetics of Ni/a-Ge reactions", *Thin Solid films*, **253** (1-2) (1994) 456-461.
- [19] S. Gaudet, C. Detavernier, C. Lavoie, and P. Desjardins, "Reaction of thin Ni films with Ge: Phase formation and texture", *J. Appl. Phys.*, **100** (2006) 034306.
- [20] L.J. Lin, K.L. Pey, W.K. Choi, E.A. Fitzgerald, D.A. Antoniadis, A.J. Pitera, M.L. Lee, D.Z. Chi and C.H. Tung, "The interfacial reaction of Ni

- with (111)Ge, (001)Si<sub>0.75</sub>Ge<sub>0.25</sub> and (100)Si at 400 °C”, *Thin Solid films*, **462-463** (2004) 151-155.
- [21] L.R. Doolittle, “A Semi-automatic Algorithm for Rutherford Backscattering Analysis”, *Nucl. Instrum. Methods Phys. Res., Sect. B*, **15** (1986) 227-231.
- [22] L.R. Doolittle, “Algorithm for rapid simulation of Rutherford Backscattering Spectra”, *Nucl. Instrum. Methods Phys. Res., Sect. B*, **9** (1985) 344.
- [23] Kanyembo J. Pondo, 2010. In situ real-time Rutherford Backscattering Spectrometry study of Ni/Ge interaction. MSc. Dissertation, University of Zambia.
- [24] P. Gas and F. M. d’Heurle, “Formation of silicide thin films by solid state reaction”, *Appl. Surf. Sci.* **73**, (1993) 153-161.
- [25] T.B. Massalski, 1986. *Binary Alloy Phase Diagrams*, American Society for Metals, Ohio: Metal Park.
- [26] Qingchun Zhang, Nan Wu, Thomas OSIPOWICZ, Lakshmi Kanta BERA and Chunxiang Zhu, “Formation and Thermal Stability of nickel germanide on germanium substrate”, *Japanese Journal of Applied Physics* **44** (45) (2005) L1389-L1391.